Integrating UAV Multi-Sensor Data for Archaeological Site Detection at Thermi, Lesvos

Asvestas Alexandros
University of Aegean
Department of Geography
Remote Sensing and GIS Research Group
Mytilene, Lesvos
asvestasal@gmail.com

Asst. Prof. Vasilakos Christos
University of Aegean
Department of Geography
Remote Sensing and GIS Research Group
Mytilene, Lesvos
chvas@aegean.gr

***Abstract*— This study employs a multi-sensor approach, combining RGB photogrammetry, LiDAR, and drone thermography, to investigate the prehistoric site of Thermi, Lesbos. RGB imagery provided high-resolution mapping, LiDAR-derived DTM identified microtopographic anomalies, and thermal imaging detected subsurface features based on thermal inertia variations. Statistical and Kernel Density Analysis revealed a correlation between thermal anomalies and architectural remains, validating the effectiveness of UAV thermography for archaeological prospection. Results emphasize the importance of adaptive flight planning, as environmental factors significantly influence thermal anomaly visibility. This study demonstrates that integrating multispectral sensors and seasonal data acquisition can further refine UAV-based archaeological surveying for enhanced precision.**

Keywords*— *UAV, Remote Sensing, Archaeology, Drone Thermography, Multispectral Sensors, Archaeological Surveying

I. Introduction

The integration of Unmanned Aerial Systems (UAVs) with advanced sensor technologies has significantly transformed archaeological survey methods. Remote Sensing enables precise and efficient detection and analysis of ancient architectural remains [1]. This study explores the integration of UAV Red Green Blue (RGB) photogrammetry, Thermal (TIR), and Light Detection and Ranging (LiDAR) data into the process of the archaeological surveying.

The case study is the prehistoric site of Thermi in Lesvos, located 10 km north of Mytilene. Inhabited from Early Bronze Age (ca. 3400 BCE) to a period contemporaneous with Troy II (ca. 2000 BCE or later) [2] Thermi was excavated between 1926 and 1931, revealing five superimposed settlements with distinct architectural and ceramic phases. These ranged from large, well-constructed towns to later settlements with more impact layouts with semi-apsidal structures. The southwestern part of the site is exposed, maintained, and open to the public, while the northeastern section was buried by W. Lamb around 1931.

II. UAV Remote sensing in archaeology

Aerial Archaeology is a specialized field within remote sensing that focuses on observing landscapes [3] to identify, confirm and analyze ancient artifacts and their spatial relationships. The practice in this field has been made easier and cost-effective by using commercially available UAVs. Equipped with high-resolution RGB, thermal and multispectral sensors, UAVs capture detailed surface characteristics, temperature variations, and vegetation indices, improving archaeological surveys.

Optimized UAV flight parameters ensure high-resolution data. Photogrammetry produces 3D models and orthomosaics for site and landscape documentation. LiDAR enables sub-canopy mapping and enhances 3D reconstructions while thermal data reveal soil anomalies linked to buried structures, and multispectral imaging shows interactions between vegetation and archaeological remains [4]. Geographic Information System (GIS) software is used for spatial analysis, risk assessment, and conservation planning of areas with cultural interest.

Despite its advantages, UAV-based remote sensing in archaeology faces challenges and debates While UAVs are cost-effective in human labor, high-end remote sensing sensors and data processing require significant investment [5]. The optimal timing for UAV surveys remains contested; post-sunset is generally preferred for thermal imaging, but studies also report midday effectiveness depending on environmental conditions [6], [7]. Furthermore, researchers debate about whether these datasets can yield reliable results as standalone methodologies or if an integration of these data is preferable for more accurate interpretations [8].

III. Methodology

A. Data Acquisition

The flight plans for data acquisition were designed based on bibliographical examples and the specifications of each UAV, and its sensors to minimize the required flights. The flight with the thermal sensor was executed on 15/11/2024 at 11:46 after a day of rainfall with a DJI Matrice 300 RTK equipped with the Zenmuse H20T. The RGB flight performed the same day at 12:27 with a DJI Mavic 3E RTK, a cloudy sky, and minimal shadowing. The LiDAR flight performed on 5/12/2024 at 10:17 with a DJI Matrice 300 RTK and a Zenmuse L1 sensor. Twenty-two Ground Control Points (GCPs) were taken to verify the UAVs RTK accuracy. The flight plans were designed through the DJI Pilot apps associated with each UAV and sensor model from their dedicated controllers.

B. Data Processing

Each dataset was photogrammetrically processed, generating georeferenced orthomosaics. The RGB photos were aligned creating a high-resolution base map with a cell size 0.019 m. The produced orthomosaic was the visual and geographical reference for the next steps of the process (**Fig. 1 A**).

LiDAR produced a raw point cloud with a 501 pts/m^2 density (**Fig. 1 B**). Using CloudCompare software, the noise was removed by applying the Statistical Outlier Removal (SOR) filter, while the Cloth Simulation Filter (CSF) [9] plugin separated ground and off-ground points. The classified ground cloud was rasterized with a grid step of 0.05m. and linear interpolation to produce a Digital Terrain Model (DTM).

Thermal dataset was pre-processed with DJI thermal SDK library to extract temperature for each image.

Subsequently, the same photogrammetric workflow applied to RGB dataset was used resulting in the generation of a thermal orthomosaic. The temperature values on the thermal orthomosaic ranged from -5.45 C^0 to 37.11 C^0, an unusually large range for both the season and the area. The most distorted thermal readings were observed in urban sections due to buildings, rooftops, and the heat emitted by vehicles. After masking these distortions, the thermal range of the area ranged from 7.5 to 30°C (**Fig.1 C**).

To quantitatively assess the thermal variations, the study area was split into three zones: a) Exposed Structures, b) Buried Structures, and c) Control areas, which are the areas where it is known that there aren't any archaeological remains. Descriptive statistics are provided for each of these area types (**Table I**).

Table 1

Regions	***Thermal Values on C^0***			
	RANGE	***MEAN***	***SD***	***CV***
Exposed Structures	15.43	16.52	2.27	13.76 %
Buried Structures	17.12	18.43	1.64	8.90 %
Control Areas	16.17	14.71	2.07	14.05 %

Pixels with abrupt 3-4 C^0 deviations from their neighbors were isolated [11] and vectorized into points. Points located in shadows or near transitional urban-natural edges were manually removed, retaining only the thermal drop points that had no apparent surface causes. A Kernel Density map was then estimated to visualize the spatial clustering of these thermal fluctuations, highlighting zones that correlated with both visible and subsurface architectural remains. Based on comparisons between Lamb's architectural plans and the surface elevation derived from the LiDAR-based DEM, the subsurface features appear to be located at a maximum depth of 50 cm.

IV. RESULTS

The RGB orthomosaic is used as a high-resolution base map. Intergrading topographical drawings of the Lesvos' Ephorate of Antiquities and the RGB dataset helped with classifying the exposed archaeological features based on the period and the settlement phases they belong to. It also served as a foundation for overlaying thermal, and LiDAR outputs, enabling cross-validation of anomalies (**Fig. 2**).

On the other hand, the surface visibility of thermal contrasts indicating buried features is influenced by several key factors, including the difference in thermal inertia between the archaeological remains and the surrounding soil [12]. The highest mean temperature was observed over Buried Structures, indicating higher thermal inertia in this zone. This supports the hypothesis that subsurface features retain heat longer than surrounding areas and create detectable anomalies in the thermal dataset. The Exposed Structures zone has a moderate temperature variation with a Mean of 16.52 C^0 but shows a higher SD at 2.27 C^0 and a CV of 14.05% due to the material variability and their direct solar exposure. The biggest variability with a CV of 14.05%, accompanied by the lowest mean temperature of 14.71 C^0 is shown in the Control Areas zone where soil moisture and vegetation are the only factors present (**Fig. 3**).

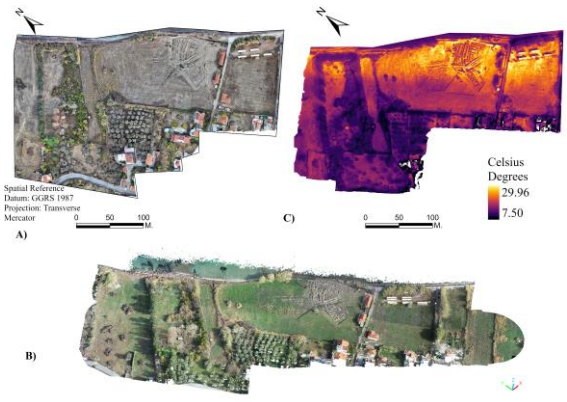

Fig. 1 A) RGB orthomosaic, B) Point Cloud from the LiDAR dataset, C) Thermal Orthomosaic.

These statistical findings provide a quantitative basis for analyzing the spatial distribution of thermal anomalies, which is further examined through Kernel Density Analysis mapping. Identifying and vectorizing the thermal anomaly points, facilitated the creation of a Kernel Density map, revealing "hotspots" with the highest concentration of thermal fluctuations (**Fig. 4**). The hotspots spatially correlated with the visible architectural remains, reinforcing that standing walls and exposed features influence local heat retention and dissipation rates. Additionally, anomalies were concentrated in the northeastern zone suggesting the presence of underlying walls and foundations, aligning with the area of known buried structures.

V. DISCUSSION

The 3-4 C^0 temperature fluctuations are consistent with previous research on thermal inertia in archaeological contexts [13]. Rainfall before data acquisition enhanced the contrast between buried structures and adjacent soils improving feature detectability. LiDAR-derived DTM with RGB orthomosaic improved the accuracy of archaeological feature identification. Subtle elevation changes, not visible through RGB alone, aligned with thermal anomalies and supported the interpretation of buried archaeological features.

This hybrid approach (RGB, LiDAR, Thermal) shows greater efficacy than relying on a single technology alone [8]. It compensates for individual weaknesses while offering a boarder perspective on the above and below ground features. Although midday flights are sometimes less favored for thermal imaging, local climate and recent precipitation here actually improved feature visibility, indicating that ideal

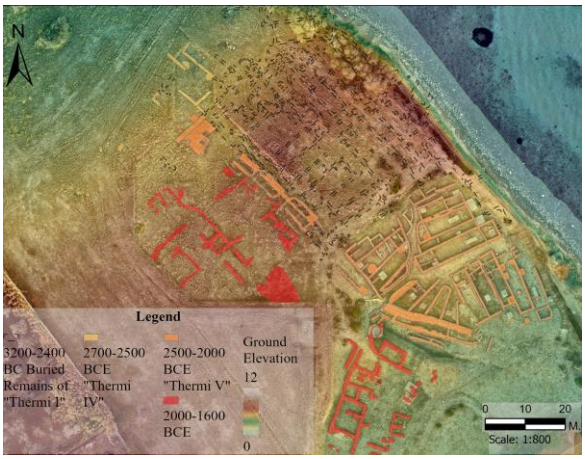

Fig. 2 RGB base map with DEM and Archaeological site Classification.

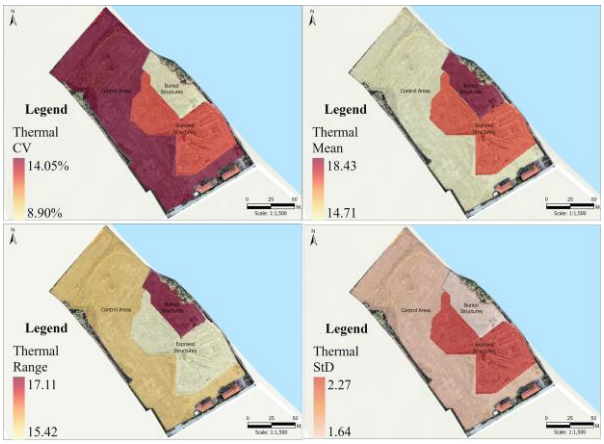

Fig. 3 Visualization of the Zonal Statistics and the Kernel Density Analysis.

flight schedules can vary based on site-specific factors.

This methodology highlights the importance of adaptive flight planning, even when unconventional, as demonstrated by climatic conditions like the post-rainfall flight executed during this research. It also shows the importance of integrating multi-sensor data. The correlation between thermal hotspots and microtopography helps mitigate misinterpretations of the results and the limitations of standalone remote sensing techniques.

V. CONCLUSIONS

A UAV-based multi-sensor data combination, adapted to local environmental conditions, can overcome single-sensor limitations in aerial archaeology. The methodology linking visible RGB data, the Law of Thermal Inertia, and subtle elevation changes provides a framework for noninvasive prospection of buried features at a depth of a maximum of 50cm from the surface.

Thermal anomalies variability are the most significant parameters to consider for locating subsurface structures. Adaptive flight planning managed to enhance the anomalies and data combination highlighted the overlapping anomalies from each sensor type. It also shows that site location and climate conditions are important factors to be considered before starting the survey process.

Further refinement is needed in automated anomaly classification. Machine learning and predictive modeling could be implemented for more reliability of thermal anomaly detection [4]. Seasonal data could also provide further insights into how environmental variables influence the visibility of subsurface structures. Integrating multispectral data can also add to the interactive relationship between vegetation and subsurface structures.

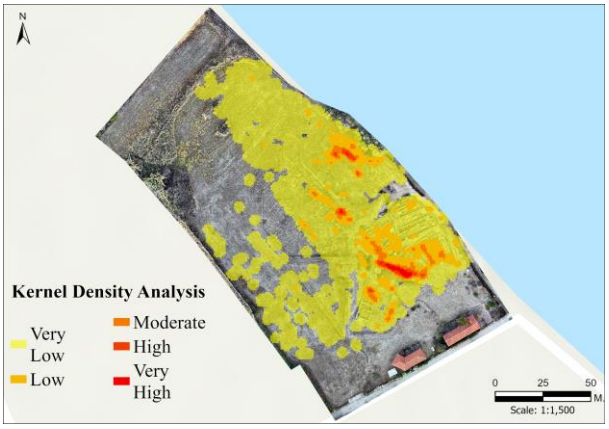

Fig. 4 Kernel Density Analysis Map.

ACKNOWLEDGMENT

Appreciation is due to Dr. Pavlos Triantafyllidis, Director of the Archaeological Ephorate of Lesvos, facilitating the necessary permissions for this study. The equipment was provided by the Cartography Lab of the University of the Aegean's Department of Geography, while Dr. Papadopoulou E. was the designated pilot, ensuring high-quality data acquisition.

REFERENCES

[1] A. Agapiou, V. Lysandrou, R. Lasaponara, N. Masini, and D. Hadjimitsis, "Study of the Variations of Archaeological Marks at Neolithic Site of Lucera, Italy Using High-Resolution Multispectral Datasets," *Remote Sensing*, vol. 8, no. 9, p. 723, Sep. 2016, doi: 10.3390/rs8090723.

[2] W. Lamb and J. K. Brock, "Excavations at Thermi," *Annu. Br. Sch. Athens*, vol. 31, pp. 148–165, Nov. 1931, doi: 10.1017/S0068245400011709.

[3] S. H. Parcak, *Satellite remote sensing for archaeology*, 1. publ. London: Routledge, 2009.

[4] A. Guyot, M. Lennon, T. Lorho, and L. Hubert-Moy, "Combined Detection and Segmentation of Archeological Structures from LiDAR Data Using a Deep Learning Approach," *Journal of Computer Applications in Archaeology*, vol. 4, no. 1, p. 1, Feb. 2021, doi: 10.5334/jcaa.64.

[5] K. Lambers *et al.*, "Combining photogrammetry and laser scanning for the recording and modelling of the Late Intermediate Period site of Pinchango Alto, Palpa, Peru," *Journal of Archaeological Science*, vol. 34, no. 10, pp. 1702–1712, Oct. 2007, doi: 10.1016/j.jas.2006.12.008.

[6] J. Waagen, J. G. Sánchez, M. Van Der Heiden, A. Kuiters, and P. Lulof, "In the Heat of the Night: Comparative Assessment of Drone Thermography at the Archaeological Sites of Acquarossa, Italy, and Siegerswoude, The Netherlands," *Drones*, vol. 6, no. 7, p. 165, Jul. 2022, doi: 10.3390/drones6070165.

[7] J. Á. Salgado Carmona, E. Quirós, V. Mayoral, and C. Charro, "Assessing the potential of multispectral and thermal UAV imagery from archaeological sites. A case study from the Iron Age hillfort of Villasviejas del Tamuja (Cáceres, Spain)," *Journal of Archaeological Science: Reports*, vol. 31, p. 102312, Jun. 2020, doi: 10.1016/j.jasrep.2020.102312.

[8] J. Hollesen, M. S. Jepsen, and H. Harmsen, "The Application of RGB, Multispectral, and Thermal Imagery to Document and Monitor Archaeological Sites in the Arctic: A Case Study from South Greenland," *Drones*, vol. 7, no. 2, p. 115, Feb. 2023, doi: 10.3390/drones7020115.

[9] W. Zhang *et al.*, "An Easy-to-Use Airborne LiDAR Data Filtering Method Based on Cloth Simulation," *Remote Sensing*, vol. 8, no. 6, p. 501, Jun. 2016, doi: 10.3390/rs8060501.

[10] J. Fernández-Hernandez, D. González-Aguilera, P. Rodríguez-Gonzálvez, and J. Mancera-Taboada, "Image-Based Modelling from Unmanned Aerial Vehicle (UAV) Photogrammetry: An Effective, Low-Cost Tool for Archaeological Applications: Image-based modelling from UAV photogrammetry," *Archaeometry*, vol. 57, no. 1, pp. 128–145, Feb. 2015, doi: 10.1111/arcm.12078.

[11] J. Casana, A. Wiewel, A. Cool, A. C. Hill, K. D. Fisher, and E. J. Laugier, "Archaeological Aerial Thermography in Theory and Practice," *Adv. archaeol. pract.*, vol. 5, no. 4, pp. 310–327, Nov. 2017, doi: 10.1017/aap.2017.23.

[12] A. C. Hill, E. J. Laugier, and J. Casana, "Archaeological Remote Sensing Using Multi-Temporal, Drone-Acquired Thermal and Near Infrared (NIR) Imagery: A Case Study at the Enfield Shaker Village, New Hampshire," *Remote Sensing*, vol. 12, no. 4, p. 690, Feb. 2020, doi: 10.3390/rs12040690.

[13] C. Kuenzer and S. Dech, Eds., *Thermal Infrared Remote Sensing: Sensors, Methods, Applications*, vol. 17. in Remote Sensing and Digital Image Processing, vol. 17. Dordrecht: Springer Netherlands, 2013. doi: 10.1007/978-94-007-6639-6.